Clinical Radiology 74 (2019) 13–28

Contents lists available at ScienceDirect

Clinical Radiology

journal homepage: www.clinicalradiologyonline.net

Review

MRA of the skin: mapping for advanced breast reconstructive surgery

N.D. Thimmappa [a,*], J.V. Vasile [b,c], C.Y. Ahn [d], J.L. Levine [c], M.R. Prince [e,f]

[a] Radiology, University of Missouri, Columbia, MO, USA
[b] Division of Plastic and Reconstructive Surgery, Northern Westchester Hospital, Mt. Kisco, USA
[c] New York Eye and Ear Infirmary of Mount Sinai, Plastic Surgery, New York, NY, USA
[d] Plastic Surgery, New York University Langone Medical Center, New York, NY, USA
[e] Radiology, New York-Presbyterian Hospital, Columbia University, NY, USA
[f] Radiology, Weill Cornell Medical Center, NY, USA

Autologous breast reconstruction using muscle-sparing free flaps are becoming increasingly popular, although microvascular free flap reconstruction has been utilised for autologous breast reconstructions for >20 years. This innovative microsurgical technique involves meticulous dissection of artery–vein bundle (perforators) responsible for perfusion of the subcutaneous fat and skin of the flap; however, due to unpredictable anatomical variations, preoperative imaging of the donor site to select appropriate perforators has become routine. Preoperative imaging also reduces operating time and enhances the surgeon's confidence in choosing the appropriate donor site for harvesting flaps. Although computed tomography angiography has been widely used for preoperative imaging, concerns over excessive exposure to ionising radiation and poor iodinated contrast agent enhancement of the intramuscular perforator course has made magnetic resonance angiography, the first choice imaging modality in our centre. Magnetic resonance angiography with specific post-processing of the images has established itself as a reliable method for mapping tiny perforator vessels. Multiple donor sites can be imaged in a single setting without concern for ionising radiation exposure. This provides anatomical information of more reconstruction donor site options, so that a surgeon can design a flap of tissue centralised around the best perforator, as well as a back-up perforator, and even a back-up flap option located on a different region of the body. This information is especially helpful in patients with a history of scar tissue from previous surgeries, where the primary choice perforator is found to be damaged or unsuitable intraoperatively. In addition, chest magnetic resonance angiography evaluates recipient site blood vessel suitability including vessel diameters, course, and branching patterns. In this article we provide a broad overview of various skin flaps, clinical indications, advantages and disadvantages of each of these flaps, basic imaging technique, along with advanced sequences for visualising tiny arteries in the groin and in the chest. Post-processing techniques, structure of the report and how automation of the reporting system improves workflow is described. We also describe applications of magnetic resonance angiography in postoperative imaging.

* Guarantor and correspondent: N. D. Thimmappa, Department of Radiology-MU, One Hospital Dr., Columbia, MO 65212, USA. Tel.: +1 5738821026.
E-mail address: tnandadeepa@gmail.com (N.D. Thimmappa).

https://doi.org/10.1016/j.crad.2017.12.018
0009-9260/

Introduction

Perforator flap surgery overview

Surgical breast reconstruction after mastectomy restores breast symmetry and hence the quality of life without affecting prognosis or impeding detection of cancer recurrence.[1,2] Good options for breast reconstruction allow more women at high risk of developing breast cancer to seriously consider prophylactic mastectomy.

Breast reconstruction can be performed using implants or autologous tissue. Silicone and saline implants may have both short- and long-term complications including infection, allergic reaction, rupture, capsular contracture, implant rippling, implant migration or implant leakage,[3] and anaplastic large cell lymphoma (ALCL).[4,5] In autologous breast reconstruction, vascularised tissue is commonly transferred from the lower abdomen (deep inferior epigastric artery [DIEA] perforator flap; DIEP), upper back (thoracodorsal artery perforator flap; TDAP), upper thigh (profunda artery perforator; PAP), or buttock (superior/inferior gluteal artery perforator artery perforator flap; SGAP/IGAP) to the chest area create a breast mound. The ideal material for reconstruction of the breast is skin and fat alone, although autologous reconstruction using myocutaneous flaps, which involve transection and removal of muscle, such as transverse rectus abdominis myocutaneous flap (TRAM) and latissimus dorsi flaps are still practised.[6] The reconstructed breast mound consisting of fat and skin quickly takes the more natural shape of the original breast from movements of the body and effects of gravity. Nerves and blood vessels slowly grow into the reconstructed breast resulting in a warm breast that may even develop sensation over time.[7] The native vasculature of these flaps arises on the deep surface of the muscle and supplies the overlying skin and fat via perforators. By dissecting these perforating artery/vein vessel bundles as they course through the muscle, flaps composed of skin and fat alone may be harvested from various regions of the body without the need for muscle removal. Advantages of this technique include no functional loss of the muscle, decreased risk of abdominal hernia, decreased postoperative pain, and a shortened hospital stay. This careful and thorough microvascular technique, however, requires long operative times. The patient and the surgeon decide on the best area to harvest tissue based on the location of the most desirable perforator and favourable distribution of subcutaneous fat.[8] If multiple options exist, patient preference is paramount in making a joint decision between patient and the surgeon.

Computed tomography (CT) or magnetic resonance imaging (MRI)-derived coordinates locate perforator relative to a reference point, e.g., umbilicus. A day before the planned surgery, skin markings are placed at the proposed flap location. A hand-held Doppler ultrasound probe is typically used to verify the location of perforators found on preoperative MR angiography (MRA) or CT angiography (CTA). Then, an elliptical-shaped donor flap is designed centred around the best perforators (Fig 1a). The skin and subcutaneous fat is elevated, and a sufficient length of perforator vascular pedicle is dissected to allow tension free anastomosis to the internal mammary vessels (Fig 1b–d). Tissue transferred to the chest wall is sculpted into a breast mound (Fig 1e and f). Donor sites that will be illustrated in this article are the lower abdomen, the upper buttock, the lower buttock, the back, and the upper thigh.

This article discusses in detail the acquisition and interpretation of MRA of the perforator flap. Different donor sites used for flap harvesting are reviewed together with relevant anatomical and surgical considerations for optimal perforator selection and avoiding potential pitfalls.

Preoperative imaging

Various imaging methods are available for preoperative imaging for perforator flap breast reconstruction.[9] Several studies have established comparable accuracy of MRA and CTA in preoperative perforator artery imaging.[10,11] High-resolution preoperative perforator flap CTA can have a radiation dose as high as 71 mSv.[11] Unfortunately, attempts to reduce CTA dose leads to reduction in CTA image quality. At our institution, MRA for preoperative imaging of perforator flaps for breast reconstruction is routinely used. CTA is performed primarily when MRA is contraindicated such as with severe claustrophobia. Most patients with claustrophobia can tolerate an MRI if an anxiolytic is prescribed.

MRA technique

The patients are asked to remove any clothing that makes an impression on the skin, especially undergarments. Vitamin E capsules, that are visible on MRA images, are placed on surface landmarks that serve as reference points for plastic surgeons, e.g., umbilicus, top of buttock crease, inferior gluteal crease, and sternal notch. The optimum reference points, patient position in the MRI machine, and coverage for different types of perforator flaps are described under the discussion of each flap type; however, as the DIEP flap is the first choice for a majority of patients, the initial positioning is generally prone to minimise motion artefact in the anterior abdominal/pelvic fat.

Scanning starts with acquisition of the three-plane localiser. Axial and coronal single shot fast spine echo (SSFSE) images are acquired next. These T2-weighted sequences screen for pathology and to help characterise any lesions seen on other sequences, e.g., enhancing lesions seen on post-gadolinium sequences. Occult metastatic disease is detected in about 4% of cases in our experience[12,13] (Fig 2). Axial three-dimensional (3D) spoiled gradient echo sequence (SPGR; liver acquisition with accelerated volume acquisition [LAVA] in the GE system) is acquired with imaging parameters of: 3.9 ms repetition time (TR)/1.9 ms echo time (TE)/15° flip angle, 125 kHz bandwidth, 3 mm section thickness reconstructed at 1.5 mm intervals using twofold zero interpolation (ZIP 2), 512×128–256 matrix, parallel acceleration factor of 2. Unenhanced imaging is important to determine the adequacy of fat suppression, especially for subcutaneous fat at the periphery of the field

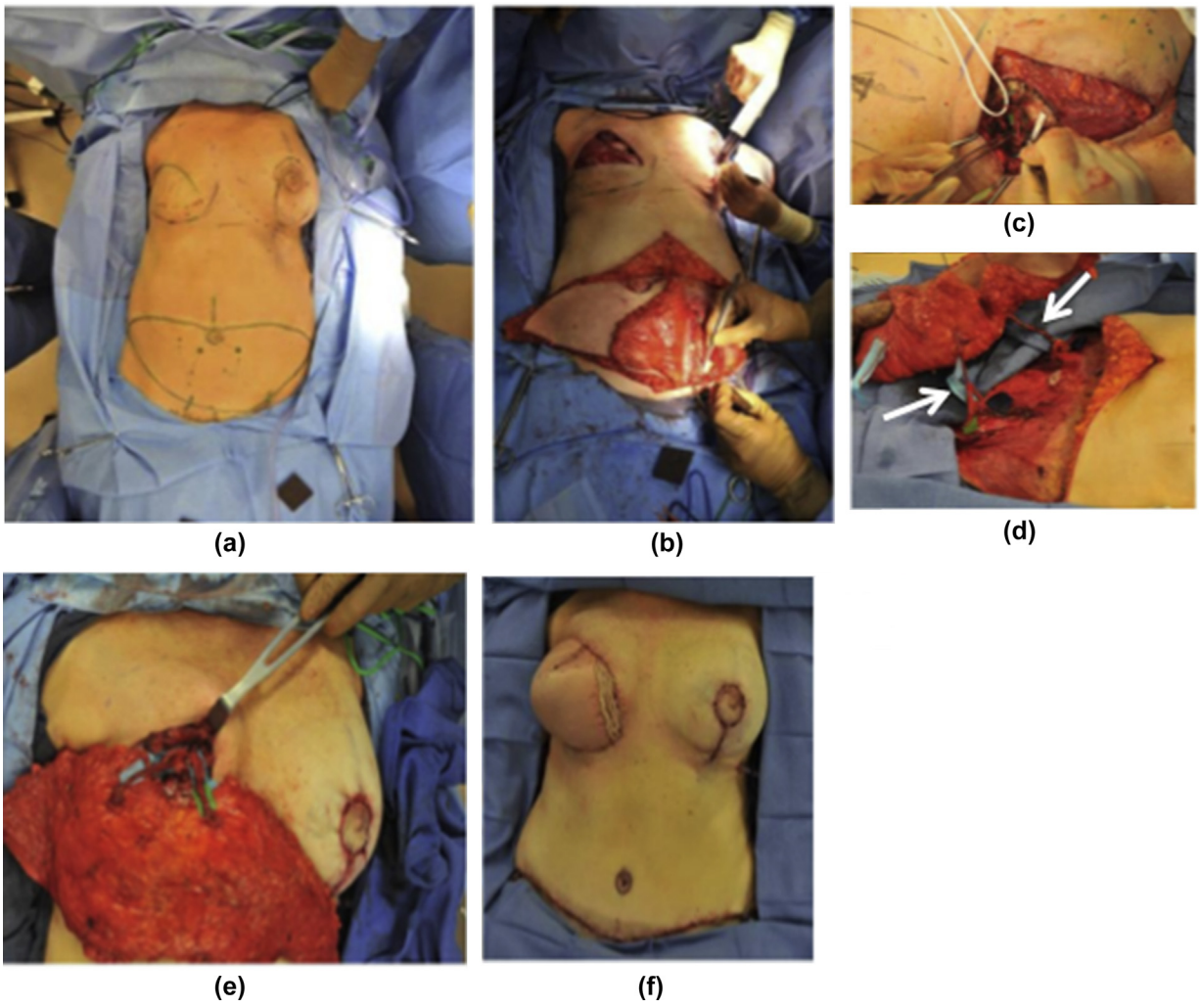

Figure 1 Perforator flap surgical technique. Perforator locations based on imaging reports and/or hand held Doppler are marked on the skin (a). Incision along the arc of the premarked elliptical design (b), simultaneously, the recipient site is prepared, the IMAs and IMVs are exposed (c), the flap is lifted with extreme caution to preserve the perforator pedicle (d) (arrows), the DIEA is anastomosed to IMA and DIEVs are anastamosed to IMVs in the chest (e), the flap is folded into a breast mound to match the contours of the contralateral breast (f).

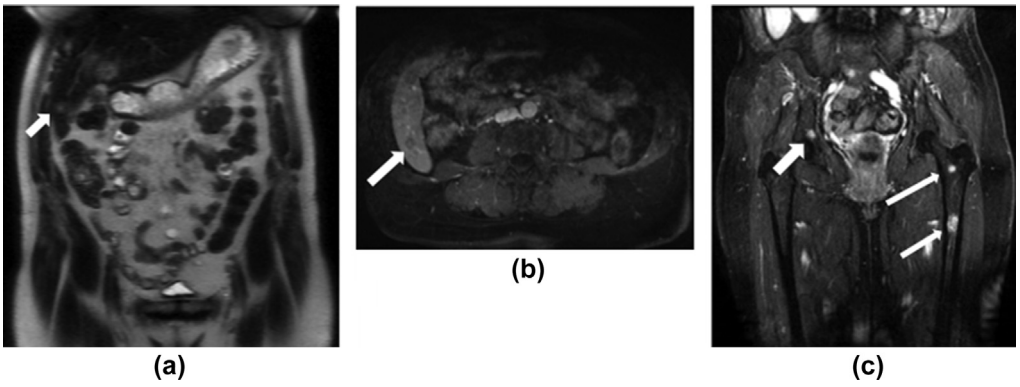

Figure 2 Incidentally noted intermediate T2-weighted lesions on pre-contrast images (a) with enhancement on post-contrast sequences (b), confirms the suspicion of metastasis. Enhancing bone metastasis in a patient with history of breast cancer, also incidentally detected on pre-operative imaging (arrows) (c).

of view and when there are metal implants, e.g., tissue expanders, which may distort the magnetic field.

Dynamic contrast imaging

The arterial phase imaging is performed using high temporal resolution multiphase imaging (e.g. DISCO), automated triggering (smartprep), or MR fluoroscopy to initiate scanning after the arrival of contrast medium in the abdominal aorta with breath-holding on inspiration. Gadobenate dimeglumine, a high relaxivity GBCA with a long vascular enhancement duration is injected at 1 ml/s followed by a saline flush at the same injection rate. Although contrast medium in both the artery and vein of the perforator bundle make visualisation easier, it is beneficial to obtain pure arterial phase images to assess the patency of the main artery, which provides the perforators. A DIEA and deep inferior epigastric vein (DIEV) may have been damaged during an abdominal surgery, such as caesarean section, appendectomy, and cholecystectomy surgeries. The DIEV may recanalise over time, giving the false impression of a patent perforator bundle on equilibrium phase images where the veins are enhancing.

Equilibrium phase imaging

The arterial phase image is immediately followed by equilibrium phase high-resolution axial 3D LAVA without parallel imaging using the following parameters: 4 ms TR/1.9 ms TE/15° flip angle, 512×512×(172–240) matrix, 125 kHz bandwidth, 3 mm section thickness reconstructed at 1.5 mm intervals using ZIP2. Phase encoding is set to the right–left (RL) direction. This is the primary sequence utilised to generate reconstructions and create reports and also serves as a reference for the plastic surgeons. It is acquired with free breathing and typically requires 3–5 minutes acquisition duration with 0.9×0.9×3 mm acquired voxel dimension and 0.9×0.9×1.5 mm reconstructed voxel dimensions (Table 1). The long scan time ensures high signal to noise ratio (SNR), and neither parallel imaging nor partial Fourier methods are used to reduce scan time. After high-resolution equilibrium phase axial imaging, a lower-resolution coronal and sagittal plane LAVA is acquired.

Table 1
Imaging technique of perforator flap angiography.

Scanner	GE signa 15.0/14.0
Patient position	Prone
Contrast	Gadofosveset trisodium
Sequences	Axial/coronal SSFSE, Axial pre, dynamic and post contrast LAVA
Key sequence	High-resolution LAVA
Imaging plane	Axial
TR/TE	4/1.9
Flip angle	15°
Slice thickness	3 mm reconstruction at 1.5 mm intervals
Matrix	512×512
Band width	125
Field of view	36–48 cm
Phase	Right to left
Coverage	Based on graft harvest site

SSFSE, shot fast spine echo; LAVA, liver acquisition with accelerated volume acquisition; TR/TE, repetition time/echo time.

After imaging the primary donor site, transverse high-resolution 3D LAVA sequences of other potential donor sites using the same parameters as above is obtained. In our experience, abdominal perforator flap imaging requires 30 minutes table time and an additional 15 minutes is allotted to any other sites that are imaged, for example, buttock, upper thigh, etc.

Other tips and tricks to further optimise image quality include: 1) patients are scanned in prone position to reduce respiratory motion in the anterior subcutaneous fat thereby eliminating the need for breath holding (Fig 3a). This allows for longer, higher resolution scans with more slices covering more anatomy. In DIEP flaps, the location (coordinates) at which the perforators exit the anterior rectus fascia in relation to the umbilical stalk attachment to the rectus fascia is unaffected by the prone position because fascia is a stable structure. The prone position is in fact optimal for visualisation of buttock perforators because the curved shape of the buttock is preserved and replicates the patient position during surgery, which increases the accuracy of the perforator coordinate locations. The supine position causes compression of the buttock tissue, resulting in a shift in the perforator coordinate location, and thus inaccuracy (Fig 3b). Exceptions to prone position are lateral thigh perforator (LTP) flap and TDAP flap imaging, where supine position is preferred as these patients are marked and operated on in the supine position. TDAP flaps may also be imaged with the side of interest elevated off the MR table using a 30° wedge and the arm on the side of interest positioned overhead, which even more closely matches the position for marking and operating. Elevating the upper arm off of the side of the chest decreases compression and shift of the perforator coordinate location, improving accuracy. It is also important for TDAP flap imaging to shift the phased array surface coils for greater coverage on the side of interest. For example, in preparation for a left TDAP flap imaging, the surface coil elements are shifted more to the patient's left side for better SNR coverage of the left thoracodorsal artery; 2) breathing and peristalsis motions can create ghosting artefacts over the anterior abdominal fat (Fig 3c). In the abdomen, phase encoding is set to RL to shift the ghosting artefacts laterally (Fig 3d). Injecting 0.5 mg glucagon intravenously just before injecting contrast agents with strong mucosal enhancement, such as gadofosveset, may aid in reducing bowel peristalsis and hence ghosting artefacts (Fig 3e). A stool softener or mild laxative to minimise bowel contents may also be helpful. If there is sufficient time, it can also be useful to repeat the acquisition with phase encoding set to anterior–posterior (AP) in order to better visualise deep circumflex iliac artery perforators. For TDAP perforators, two acquisitions are generally necessary, one with phase-encoding AP and the other with phase–encoding RL to see the full range of possible TDAP perforators without cardiac motion artefact; 3) for inhomogeneous fat suppression at the edge of the field of view, especially in patients with large body habitus, scanning at 1.5 T is preferred (Fig 3f). A two-point Dixon technique (LAVA-flex in GE system) reconstructs fat and water separately with a water only image that generally has more complete and

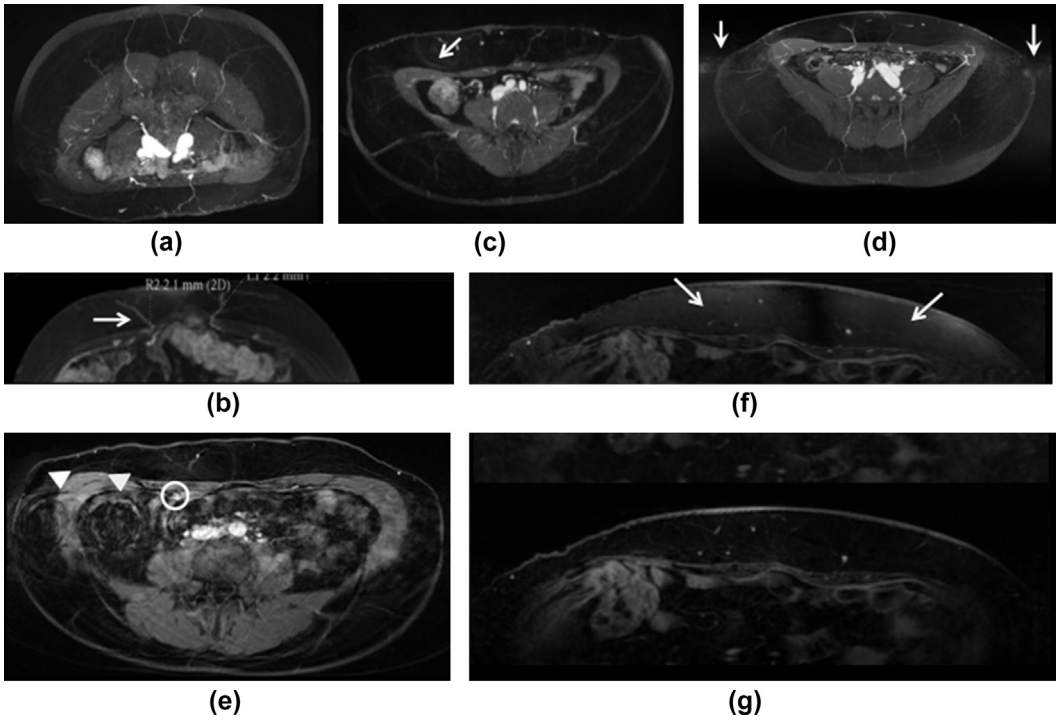

Figure 3 Optimising image quality: effect of prone (a) versus supine (b) position on visualisation of perforators in anterior abdominal wall. Note the effect of breathing motion on the anterior abdomen causing blurring of the vessels in the abdominal fat in the supine position (arrow); this also gives inaccurate diameter measurement. There could also be shift in the coordinates for the location of perforator exit sites on the fascia. (d) When phase is set RL the anterior abdominal wall is homogeneous without overlapping phase artefacts (arrows) making identification of perforator exit sites easier (d). Compare this with phase artefacts (arrows) overlapping abdominal fat in image (c). Artefacts from bowel peristalsis in image e (arrowheads) almost overlaps the DIEA and vein (encircled). Inhomogeneous fat suppression on 3D SPGR images (arrows) (f). Compare with the homogenous fat suppression on "water only" images obtained by two-point Dixon method (g). The vessels at the muscle–fat interface are seen well with the two-point Dixon method (LAVA Flex) images.

homogeneous elimination of fat signal compared to using fat saturation or inversion pulses with nearly the same data acquisition time. Perforators and their intramuscular course are well visualised on these water-only sequences (Fig 3g). State of the art 3 T systems employing the in- and out-of-phase dual- or triple-echo fat signal elimination methods with a large field of view phased array coils may be more challenging because the shorter out-of-phase TE may not allow sufficient time to acquire 512 frequency encoding steps. Imaging at 3 T will also not be acceptable for patients with tissue expanders, which represent about 10% of our cases; 4) a flip angle of 15° combined with fat suppression is helpful to delineate the fat–muscle boundary and intramuscular perforator course; 5) blood-pool or intravascular agents, such as gadofosveset trisodium, reversibly bind with albumin, similar to gadobenate dimeglumine but with a higher (90%) binding fraction. This prolongs the intravascular half-life of gadofosveset, and thus allowing for imaging of multiple regions in the same examination. The property of binding to albumin also indirectly increases T1 relaxivity by five-to sixfold. The blood pool distribution of gadofosveset is of great benefit while visualising the intramuscular course of small perforators. The added benefit of greater SNR per unit of gadolinium requires lower injection volumes[14,15]; however, with the recent withdrawal of gadofosveset from the market, we have found the gadobenate dimeglumine is nearly as good, but lasts for only about 15 minutes. This necessitates imaging each station quickly to ensure all stations are completed while gadobenate is still intravascular, and it may also be necessary to eliminate the arterial phase. Another possible blood pool contrast agent to consider is ferumoxytol but its use for MRA is considered to be off-label.

Post-processing

T2-weighted images (SSFSE sequence) and pre- and post-contrast images are reviewed to identify any pathology and help characterise enhancing lesions. An enhancing lesion carries a high suspicion of metastasis in this patient demographic (Fig 2). Arterial phase images (if obtained) are reviewed to confirm patency of the DIEA and to evaluate the presence or absence of each superficial inferior epigastric artery (SIEA). High-resolution equilibrium phase images are used for evaluating the deep inferior epigastric artery/vein all the way down to the insertion on the external iliac vessels and calculating perforator coordinates. Transverse high spatial resolution images are loaded on a computer workstation (GE Advantage Windows 4.4, Milwaukee, WI, USA), which generates coronal, sagittal, and surface-rendered reformatted images. The area of interest extends from 4 cm above the level of umbilicus to about 10–15 cm below it. The coordinates for the reference point is noted as well as the coordinates of a few large calibre perforator

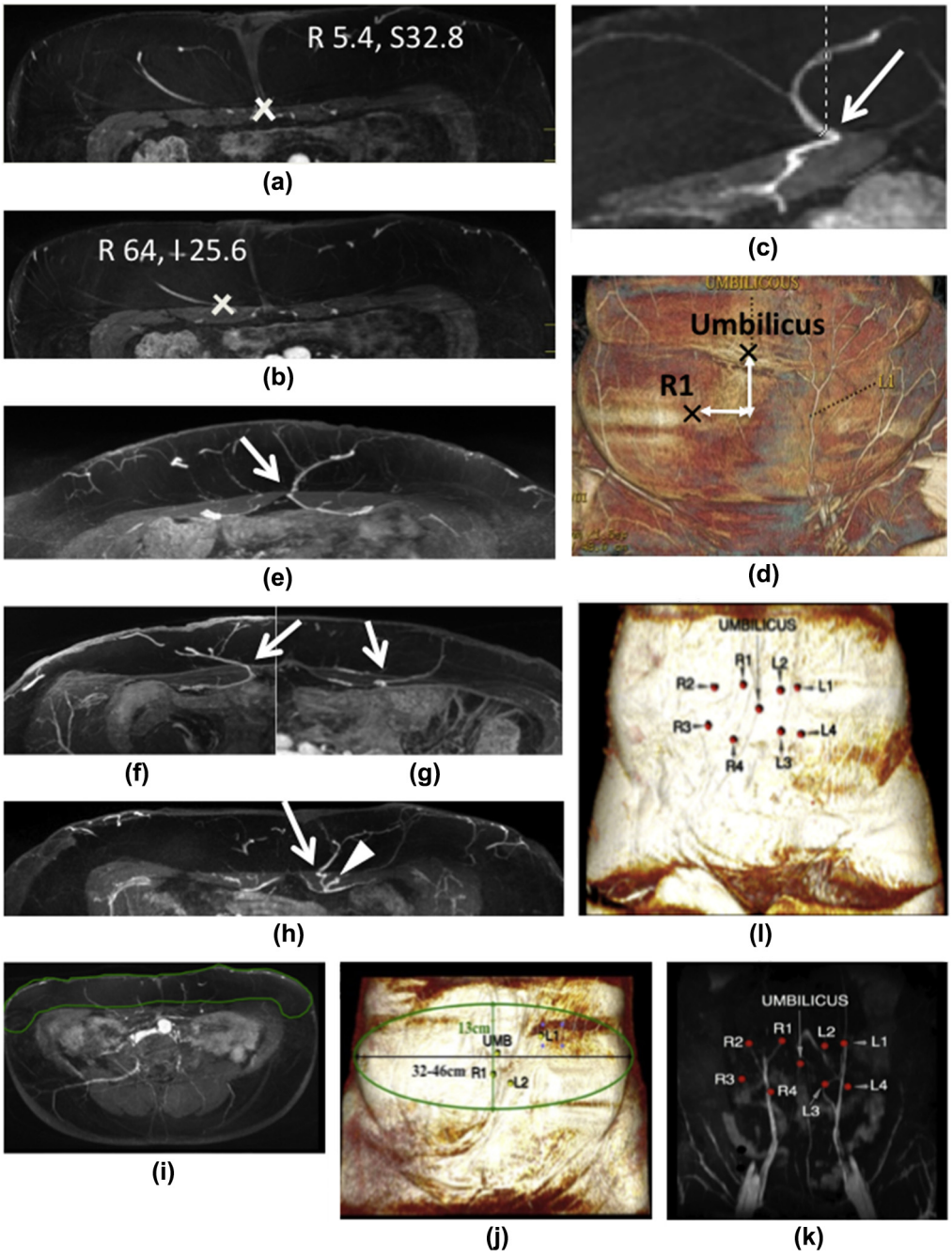

Figure 4 Post-processing the post-contrast high-resolution SPGR axial images. The co-ordinates for the reference point (x mark) (a) and individual perforators at muscle fat interface (x mark) (b) allows us to estimate the location of the perforator in relation to the reference point (c). (d) The diameter is calculated at the site of exit of the perforator from the fascia covering the muscle (arrow). Favoured intramuscular courses (arrows) are paramuscular (e), short (f), or smooth (g) trajectories. (h) Challenging courses include: tortuous course, or perforators giving of multiple intra muscular courses after coming off the origin artery (arrowheads). (i,j) An estimated flap volume is calculated by assuming an elliptical geometry and full abdominal fat thickness on a section by section basis. (k,l) Finally the perforators are superimposed on MIP and surface rendered images.

arteries at the site of exit from rectus fascia to subcutaneous fat are noted. These coordinates are used to calculate the superior/inferior and RL distance and location of each large perforator in relation to the reference point (Fig 4a–c). Simultaneously, the diameter of individual artery/vein bundles at the exit site of the artery through the superficial fascia is noted (Fig 4d). These coordinates are essential for the plastic surgeon to locate the perforators during preoperative surface marking and intra-operatively.

The perforator course, after taking off from the main artery can be paramuscular (septocutaneous; Fig 4e) or intramuscular (Fig 4f–h). A tortuous intramuscular course

hints at complicated dissection (Fig 4h). The intramuscular path is described, providing a road map for surgeons doing the dissection. For example, the first described perforator on the right "R1′, courses medial, posterior and inferior for 62 mm to reach the main trunk of DIEA". This measurement gives an estimate of vascular pedicle length.

A predicted flap volume is calculated by manual tracing on individual sections that extend through a 13 cm long segment of anterior abdominal fat, assuming an 13×36–42 cm elliptical geometry (Fig 4i and j). The lateral dimensions do not extend beyond the mid axillary lines. It is important to save a screen shot of the flap for which the volume is calculated so the surgeon can readily expand or reduce the flap dimensions to increase or reduce the volume as necessary.

3D volume-rendered images and coronal 3D maximum intensity projection (MIP) images with superimposed co-ordinates identifying the location of the perforating arteries are saved. MIP images are useful in evaluating the patency and branching pattern of DIEA (Fig 4k,l). Ideally, saved screenshots are incorporated into the final report.

Characteristics of an optimal perforator vessel

An optimal perforator is a large calibre vessel that is located centrally on the planned flap, and has a branching pattern in the subcutaneous fat of the planned flap. Being located centrally on the planned flap is advantageous because the fat closest to the perforator is perfused better.

An arterial diameter ≥1mm or a vascular bundle (artery and vein together) of ≥2 mm are the minimum requirements for a perforator to be reported. Although the "perforator diameter" indicates a combined artery and vein diameter, dynamic arterial enhancement images can confirm patency of the DIEA and assist in excluding very narrow arteries.

The ideal vessel course, if available, is a paramuscular course where a perforator courses around the rectus abdominis muscle, may be advantageous because a muscle dissection is avoided. Usually a more direct, non-tortuous intramuscular course allows for an easier dissection. A less direct course may result in a longer pedicle (Fig 4e–g). A pedicle length of at least 6 cm is favoured to allow room for anastomosis to the recipient vessels. A perforator is dissected up to its origin from a major artery, (e.g., DIEA). In a DIEP flap, a segment of DIEA is removed with the perforator, so the length of a pedicle is calculated by measuring the length of a perforator with the DIEA until its origin from the external iliac artery.

Discussion on donor site selection, perforator anatomy, and imaging pearls relevant to each location

The factors that influence a particular donor site choice are 1) patient preference: most patients have preconceived ideas regarding body image and areas which they consider their "best feature", i.e., buttocks, lateral thigh areas that they wish to preserve; 2) contraindication to use a donor site: for example, a DIEP flap may be a less favourable option in a patient with a history of multiple caesarean sections, previous abdominoplasty after weight loss/caesarean section or other abdominal surgery, or extensive liposuction; 3) fat thickness/volume: for unilateral DIEP reconstructions where volume may be an issue, the "stacked method" may be utilised or later augmented with autologous fat graft; 4) anatomy of available perforators: this may determine the surgeon's choices regarding the most to least appropriate sites and allow second options intraoperatively, should another donor site be deemed necessary (for any reason).

Usually the first choice donor site is the lower anterior abdomen (DIEP) due to favourable aesthetic results, relative abundance of fat deposited, and a long pedicle with a large diameter. Non-abdominal donor sites may be chosen by the surgeon and patient if the abdominal fat is not available due to previous abdominoplasty, history of extensive abdominal liposuction, transected vessels, or greater abundance of fat in non-abdominal donor sites (pear-shaped fat distribution). The second choice option is usually the PAP of the upper posteromedial thighs due to an adequate flap pedicle length and avoidance of turning a patient during surgery (i.e., prone position in buttock flaps and lateral decubitus position in back flaps). Turning the patient intraoperatively adds operating time as it is not possible to work on the donor site and recipient site on the chest simultaneously. Posterior thigh flaps are harvested with a patient in a supine position, with the legs frog-legged.

Visualising the vascular anatomy of many donor sites in one study is a major advantage of MRA, and is especially pertinent for the following situations: 1) when there is immediate postoperative flap failure and the surgeon needs to harvest another donor site immediately in the operating room; 2) when a patient has a history of previous surgery at a donor site (e.g., caesarean section, appendectomy or exploratory laparotomy); 3) to compare fat thickness of donor sites: when there are specific minimal volume requirements; and 4) most importantly, to enable a patient and surgeon to select the best donor site based on the fat volume and quality of perforators.

Hence, visualising multiple donor sites with a preoperative MRA influences the anatomical region selected for the donor site, confirms the vascular anatomy in patients with a history of surgeries at donor sites, and provides information for immediate back-up flap harvest with initial flap failure.

Lower abdomen

DIEP and SIEA perforator flaps

DIEP flaps are the most commonly harvested perforator flaps worldwide. A large calibre SIEA is another option when a DIEA is transected, scarred, or provides inadequate perfusion. A SIEA dissection is less traumatic to the donor site because it does not require opening of the muscle sheath and intramuscular dissection; however, there are disadvantages to an SIEA flap. A SIEA is usually smaller in diameter compared to DIEA, resulting in a size mismatch between the SIEA and the

Figure 5 DIEA anatomy on sagittal contrast images and branching pattern. The DIEA and DIEV arise from the external iliac vessels. (a) Ascends up along the sub-peritoneum before entering the rectus abdominus muscle and subsequently gives of branches that "perforate" the rectus fascia (arrow). (b) They can continue as single trunk (type 1), bifurcate (type 2), or trifurcate (type 3).

recipient artery (e.g., internal mammary artery [IMA]), which may result in a more difficult microsurgical anastomosis and arterial thrombosis.[16] A SIEA is typically located on the inferior edge of the lower abdominal flap and results in a shorter pedicle, which may make it more challenging for positioning the flap under the breast skin. The medial and typically thicker fat on the flap may not be perfused by a SIEA, leading to a smaller flap and/or fat necrosis. In addition, a SIEA harvest may result in an inguinal depression.

Perforator anatomy. The inferior epigastric arteries provide the dominant vascular supply to the lower anterior abdominal wall, and are composed of a deep and superficial system. It arises medially from the distal external iliac artery, immediately above the inguinal ligament, and ascends upward in the subperitoneal tissue. After piercing the transversalis fascia, it passes between the rectus abdominis muscle and the posterior lamella of rectus sheath (Fig 5a). Three different DIEA branching patterns have been described: type 1: a single trunk, type 2: bifurcation into a medial and lateral branch (most common), and type 3: three or more branches (Fig 5b). A surgeon looks at the branching pattern when using multiple flaps to reconstruct one breast (stacked flaps). It is possible to connect a flap pedicle to a branch of another flap pedicle so that one flap pedicle perfuses the other flap. As the DIEA branches cephalad, it gives rise to branches that perforate the rectus abdominis muscle, and supply the anterior abdominal subcutaneous fat and skin. DIEA perforating branches arising from a medial branch are called medial row perforators. Similarly perforators arising from a lateral branch of DIEA are called lateral row perforators. A pair of venae comitantes runs alongside the major branches of the DIEA within or deep to the rectus abdominis muscle (Figs 4k and 5b). A point to note is that, the medial row perforators can supply subcutaneous tissue across the abdominal midline via a subdermal plexus,[17,18] which may be an optimal perforator in unilateral reconstruction to perfuse the thicker central lower abdominal fat. The branches crossing the midline can be well visualised on thick-slab coronal MIP images, especially when a blood pool contrast agent that gives superior vessel to background contrast is used. Knowledge of arborisation patterns can help design better perfused flaps.

The SIEA has inconsistent anatomy and is absent in one third of patients. It arises from the common femoral artery, 2–3 cm below the inguinal ligament. It passes superiorly and laterally from the femoral triangle to cross the inguinal ligament. Above the inguinal ligament the SIEA penetrates Scarpa's fascia, and branches in the subcutaneous fat, anterior to the recuts sheath. A larger calibre SIEA, especially with a common origin with a superficial circumflex iliac artery provides a larger calibre vascular pedicle for microsurgical anastomosis.[10,19]

Intraoperative venous congestion of a free abdominal flap during breast reconstruction is a potential complication, with an incidence of 2.8% or higher.[20] It most commonly occurs from compression of the veins at the venous anastomosis. Rarely, venous congestion can be caused by a dominant superficial inferior epigastric venous system and deep inferior epigastric perforators that are not connected to the superficial venous system.[21,22] Hence, the anatomy of the superficial inferior epigastric vein (SIEV) is viewed (Fig 6a), and the MRA report includes the coordinate location of a large SIEV at 10 and 12 cm caudal to the umbilicus (Fig 6b). The SIEV is located superficial to Scarpa's fascia. It has a single trunk in the majority of the cases (82%). It may also bifurcate with two tributaries (17%) or rarely trifurcate (1%). The SIEV drains into the superficial femoral vein (41%) or saphenous bulb (49%) and occasionally into the long saphenous vein (12.5%).[21] The SIEV communicates with the deep venous system through perforator venae comitantes of the deep inferior epigastric vein.

Imaging for DIEP and SIEA flaps. Landmark: umbilical stalk attachment to anterior rectus fascia (Fig 4). Position: prone (Fig 3a). Coverage: 5 cm above umbilicus to pubic

symphysis. Arterial phase MRA can be used to visualise DIEA when an injury is suspected and for visualisation of small calibre SIEA (Fig 7).

Reporting DIEP and SIEA flaps. Typically, a DIEP flap is a 12 cm (cephalad to caudal) × 36–46 cm (transversely oriented) elliptical flap, extending <3 cm above umbilicus. The cephalad–caudal dimension can be increased in a patient with a large pannus and decreased in a nulliparous patient without a pannus. The lateral extensions are flexible, but typically the perfusion of subcutaneous fat is not reliable lateral to the mid-axillary line. A flap is designed on surface rendered images and an estimated flap volume is calculated using a 3D post-processing computer workstation.

The report should include the DIEA branching pattern. The branching pattern is best identified in the coronal MIP image (Fig 4k). The larger perforators on both sides of the umbilicus are identified and described using the post contrast axial high resolution images.

The following points must be mentioned while reporting SIEA: present or absent, whether it originates as a common trunk with superficial circumflex iliac artery (in this case the vessel calibre is larger and more favourable) and which series/images show this vessel so the surgeon can see it preoperatively.

Reporting the horizontal distance of SIEV from midline, 10 and 12 cm inferior to umbilicus helps the surgeons to preserve it during dissection so that it can be an ancillary venous drainage in the event the flap appears congested.

Deep circumflex iliac artery perforator flap

The lateral lower abdominal/flank fat is perfused by the deep circumflex iliac artery, superficial circumflex iliac artery, and lumbar perforators. When the anterior abdomen (DIEP flap) fat is not sufficient volume or skin for reconstruction, this lateral fat can be harvested and perfused by

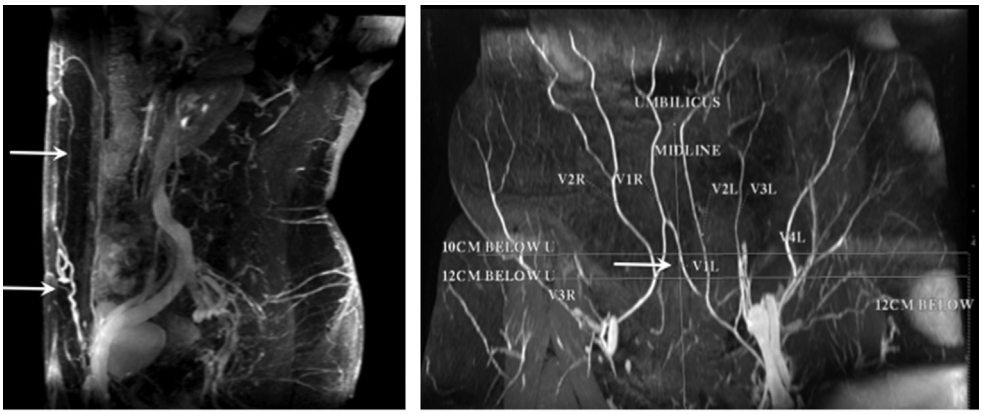

Figure 6 SIEVs demonstrate communication with the deep veins (a) (arrows) can be larger than the deep inferior epigastric veins and cross over the midline (b) (arrows). (b) Reporting the location of the vessels along the expected incision lines: 10 and 12 cm below umbilicus prevents accidental damage and bleeding, especially if the vessels are large.

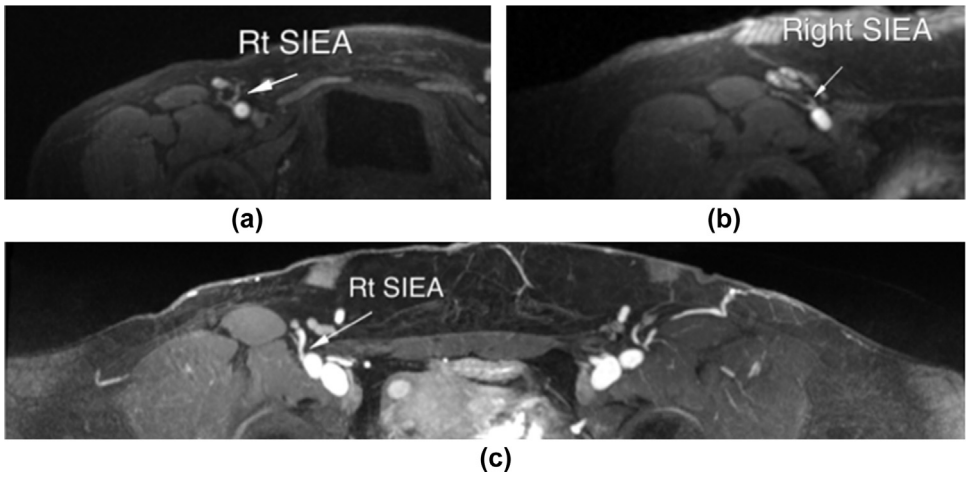

Figure 7 SIEA coming off the common femoral artery either as a common trunk with superficial circumflex iliac artery (a) or separate origins (b) is well visualised on the dynamic arterial phase images obtained using spiral K space acquisition and sliding window reconstruction. (c) Compare with the intermediate phase images with filling in both artery and vein.

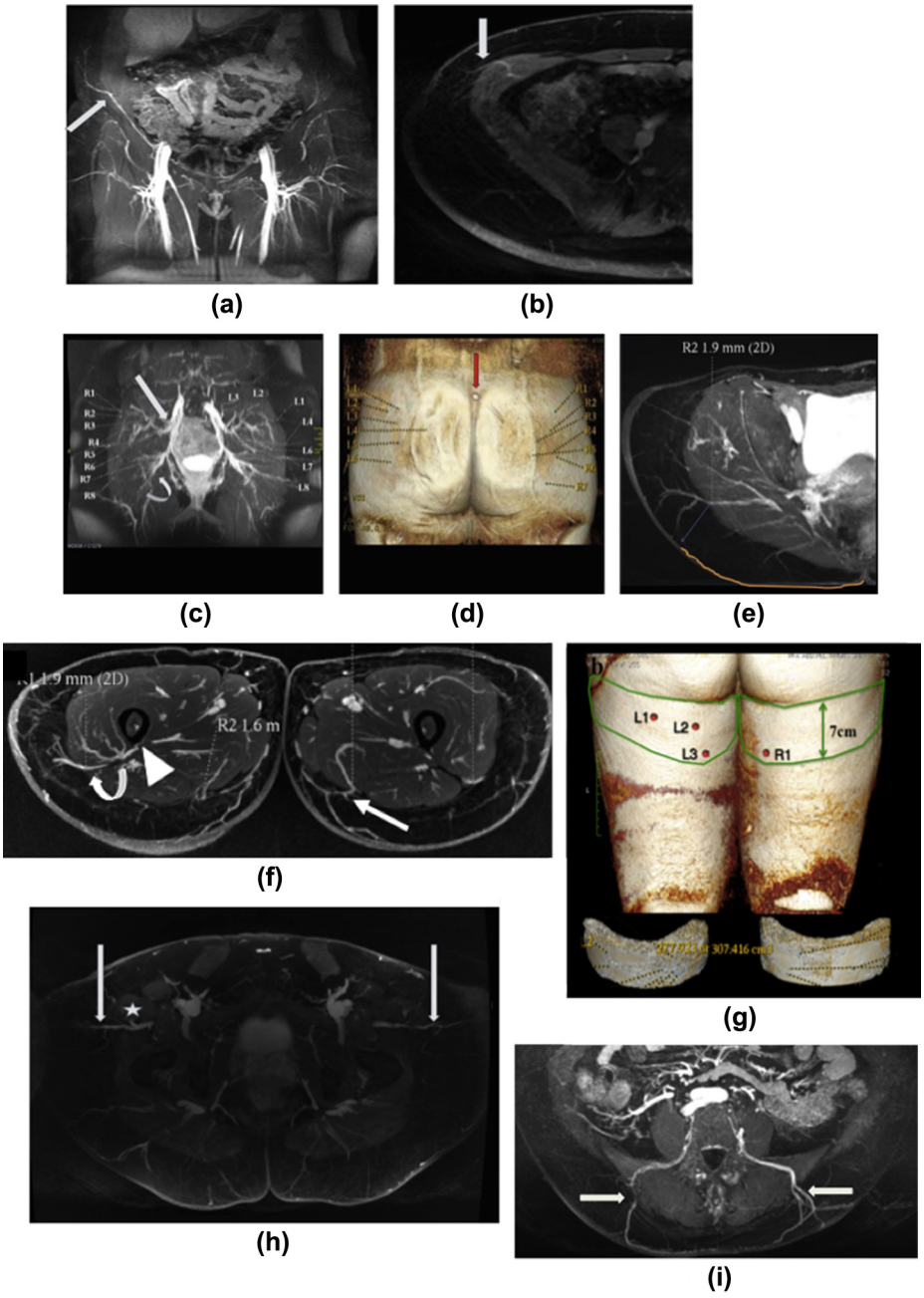

Figure 8 Non-DIEP flap options. (a) Deep circumflex iliac artery lateral course (arrow) after it comes off the external iliac artery. (b) The perforator (arrow) after piercing the traversalis fascia supplies skin and fat over the lateral flank. (c) SGAP/IGAP; Coronal MIP images of SGA (arrow), IGA (curved arrow) and the perforators coming off them. (d) A vitamin E marker is placed on the superior gluteal crease for easy identification of the landmark on the axial MRI images (arrow). (e) For calculating the lateral co-ordinates from the midline, manual tracing along the curved gluteal surface from midline is done (orange line). (f) PAP: axial thick slab LAVA images of and medial (arrow) and lateral row (curved arrow) profunda perforators. The lateral perforators can track very close to the periosteum shaft and are usually avoided (arrowhead). (g) Fat volume of a 7×22–36 cm oval is calculated bilaterally. (h) Lateral circumflex femoral artery perforator (arrow) coursing around the tensor fasciae lata (star). (i) Bilateral lumbar arteries (arrows) after arising from aorta, run posterolaterally and perforate the thoracolumbar/lumbosacral to enter the subcutaneous tissue of lower back.

an additional pedicle. The deep circumflex iliac artery may have a diameter similar to a branch of the DIEA, facilitating successful anastomosis and perfusion. There is an added potential benefit of improved aesthetic contour as the lateral fat is removed adjacent to the anterior fat, similar to circumferential torso lifts (Fig 8a and b).[23–26]

The DCIA comes off external iliac artery and travels laterally along the medial surface of the ilium. The artery then travels superficially, piercing the transversalis fascia. After giving off an ascending branch, which supplies the muscle of the abdominal wall, the DCIA continues as lateral branch, supplying the iliac crest, pierces the internal and

external oblique muscles and supplies the overlying skin. The dominant perforator can be found 1–2 cm superior and 1–4 cm lateral to the anterior superior iliac spine in clinical cases. The DCIA perforator is a good calibre vessel and is predictably present making it a valuable potential addition to DIEP.[27]

The scanning imaging coverage, position, and landmarks are the same as a DIEP flap; however, an additional acquisition with the phase encoding set anterior/posterior is done to minimise the lateral extent of bowel peristalsis motion artefacts.

Upper and lower buttock area

SGAP and IGAP flaps

Buttock perforator flaps preserve the gluteus maximus and gluteus medius muscles. An upper buttock tissue flap is based on SGAP. An inferior buttock tissue flap is based on IGAPs.

Anatomy. The superior and inferior gluteal arteries (SGA and IGA) are terminal branches of posterior division of internal iliac artery. They both exit the pelvis through the greater sciatic foramen. The SGA passes superior to the piriformis muscle and the IGA passes inferior to the piriformis. The SGA gives off intramuscular branches supplying the upper half of gluteus maximus, gluteus medius muscles and perforating branches to overlying skin and subcutaneous fat. The IGA is accompanied by the internal pudendal vessel and nerve, and the posterior femoral cutaneous nerve. It gives off perforators to the lower half of gluteus maximus muscle and overlying skin and subcutaneous fat (Fig 8c).[28,29]

Imaging SGAP/IGAP flaps. Landmark: top of the midline gluteal crease (superior gluteal crease). A vitamin E capsule is placed on top of the gluteal crease to mark this spot for precise identification on the images. Position: prone. Coverage: 5 cm above superior gluteal crease to a few centimetres below inferior gluteal crease (Fig 8d). Typically, this area is already included in the DIEP study.

Reporting SGAP/IGAP flaps. The top of the midline gluteal cleft is used as the landmark for cephalad-caudal coordinates. Manual tracing along the gluteal skin surface from the midline is used for RL coordinates (Fig 8e). The largest SGA and IGA perforators are described. Laterally located perforators and perforators with a less direct course are advantageous because they yield a longer vascular pedicle.

A predicted flap volume is calculated by manual tracing an elliptical shaped pattern extending 6 cm in the cephalad-caudal dimension and about 20–22 cm in the transverse dimension. It is important to save a screen shot of the flap for which the volume is calculated so the surgeon can view the flap design measurements.

Upper thigh

PAP flaps

A muscle sparing thigh flap, based on the PAPs is the second most popular flap harvested at our institution.[12] The PAP flap uses excess subcutaneous fat from the upper inner and posterior thigh adjacent to the buttock crease and does not harvest muscle,[30] in contrast to the transverse upper gracilis (TUG) flap which sacrifices the gracilis muscle.

Anatomy. The profunda femoris artery is a branch of the common femoral artery. It travels down the thigh close to the femur in the posterior compartment of the thigh and gives medial and lateral branches. There are usually three perforating branches. The first perforating artery gives branches to the adductor magnus and gracilis, and the second and third perforating arteries supply the semimembranosus, biceps femoris and vastus lateralis muscles. These branches further divided into musculocutaneous or paramuscular perforators.[31] Perforators that branch posterior-medially are preferred because dissection of the medial perforators can be performed with a patient in the supine position and the patient's position in the operating room does not need to be changed for breast reconstruction in the chest[30] (Fig 8f). Perforators that branch posterior-laterally are adjacent to the femoral shaft, resulting in a difficult dissection (Fig 8f).

Imaging PAP flap. Landmarks: inferior gluteal crease at the midline. Position: prone. Coverage: mid-gluteal region to 12 cm below inferior gluteal crease.

Reporting PAP flap. The mid-portion of the inferior gluteal crease is identified on the 3D surface-rendered image and the exact slice corresponding to the landmark is identified on the 3D workstation. The cephalad–caudal location of a perforator is calculated with respect to this point on the inferior gluteal crease. Similarly, the RL location is calculated with respect to a straight line along the medial border of the thigh. It is also useful to state how many millimetres posterior to the posterior border of the gracilis muscle the perforator is located to facilitate intra operative identification of perforators.

It is important not to misidentify and erroneously report caudally located inferior gluteal perforators as profunda perforators because dissection of these perforators up into the gluteal muscle will be challenging with the patient in the supine position. Occasionally, a large medial circumflex femoral artery perforator is identified perforating through the gracilis muscle. A surgeon can harvest this perforator without removing the gracilis muscle, but the lateral posterior thigh fat may not have adequate perfusion. A predicted flap volume is calculated by manual tracing an elliptical-shaped pattern from the inferior gluteal crease to 6 cm caudally, and about 20–22 cm in the transverse dimension (Fig 8g). It is important to save a screen shot of the flap for which the volume is calculated so the surgeon can view the flap design measurements.

Lateral upper thigh perforator flap

The lateral portion of the upper thigh may have a favourable fat deposition, and is perfused by lateral circumflex femoral artery perforators. The perforators course anterior and posterior around the tensor fascia latae muscle. Perforators traversing in the posterior tensor fascia latae septum will yield a slightly longer pedicle and are

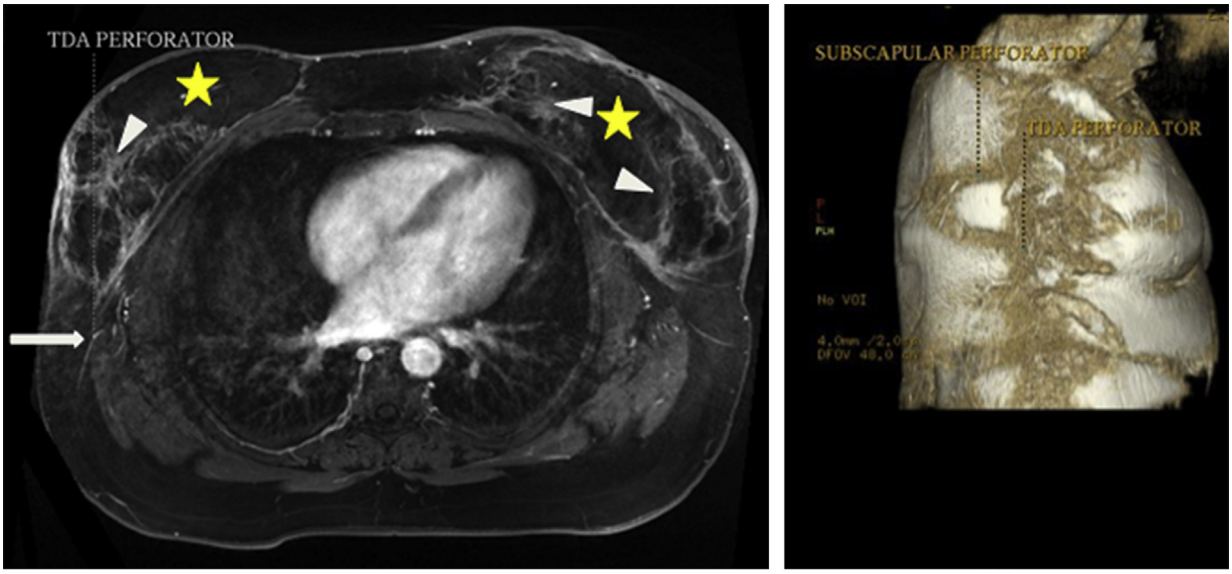

Figure 9 (a) Axial post-contrast high-resolution LAVA image of the chest in a patient who has undergone bilateral autologous breast reconstruction (star), note areas of fat necrosis (arrowheads) bilaterally. A TDAP (arrow) in the right lateral chest provides excellent option for a thoracodorsal flap with pedicle for repairing the defects. (b) Surface rendered images give co-ordinates to the location of perforator and also show the exact position of the arm during scanning raised above the head in this case.

better located in the planned flap. The perforators are measured using the umbilicus as a reference point. It may also be helpful to include the distance cephalad and caudal from the pubic tubercle. The patients are marked and operated on in the supine position. Thus, the measurements should be obtained from the supine position images. A predicted flap measurement can be calculated of the upper lateral thigh fat, using dimensions of 6×20–22 cm (Fig 8h).[24]

Lower back

The lumbar artery perforator (LAP) flap

LAP flaps utilise subcutaneous fat and skin from the lumbar region above the buttock. The LAPs are intermuscular and pass between the erector spinae and quadratus lumborum muscles.[32] The pedicle length is typically shorter when compared to other donor sites and the artery can be very close to exiting spinal nerves (Fig 8i).

Imaging and reporting LAP. Landmark: superior gluteal crease. Position: prone. Coverage: mid-buttock to upper lumbar area. The LAP flap is usually reserved for a patient without other donor site flap options.

Upper back

TDAP flap

TDAP subcutaneous fat and skin overlying the latissimus dorsi muscle, and does not remove the latissimus dorsi muscle. The thoracodorsal artery comes off the subscapularis artery, passes beneath the latissimus dorsi muscle and gives off the serratus anterior artery branch before bifurcating into a transverse and vertical branch. These branches give rise to perforators supplying the overlying skin[33] (Fig 9a).

Imaging and reporting TDAP. Landmark: sternal notch. Position: supine with hands resting on the head and the upper arm abducted to avoid compression of the lateral chest soft tissue. Axial post-contrast equilibrium sequence is obtained in lateral decubitus position to assist surgeons in marking the more posterior perforators. Coverage: sternal notch to xiphoid process. 3D surface rendered images demonstrating the exact position of the arm during the study (raised above the head or on the side) is included in the report. This information is important because the co-ordinates of individual TDAPs through the superficial fascia measured from the reference point (sternal notch) change with changes in patient positioning and arm positioning. The patient will require additional post contrast imaging sequences in a slight (30–45° degrees tilted) lateral decubitus position with the arm on the side of interest raised in order to accurately view and locate more posteriorly positioned perforators and to mimic the patient positioning intraoperatively. The report should include perforator locations in the supine and lateral decubitus positions and specify from which patient positions the perforator co-ordinates are derived[24] (Fig 9b). Sometimes, a large intercostal artery perforator can be identified at about the level of the inframammary fold and should be measured. Caudally located perforators will yield a longer pedicle length and are advantageous. Perforators that course around the latissimus dorsi muscle also are advantageous. These flaps can have a pedicle (not disconnected and anastomosed microsurgically) or free flaps. They are not usually used to reconstruct an entire breast because of less fat deposition on the upper back than the abdomen, thigh, and buttock. They are more commonly used to correct defects in a reconstructed breast (e.g., after lumpectomy or to

add volume to a reconstructed breast (Fig 9a). A predicted flap measurement can be calculated of mid upper back, using dimensions of 6×20–22 cm.

Imaging internal thoracic (mammary) arteries and veins

The internal mammary vessels are the most common recipient vessels in free flap breast reconstruction.[34] Studies have shown that the internal mammary vessels can be reliably used in almost all microsurgical candidates with low rates of vascular complications.[35]

Advantages of using the internal mammary system include its availability, particularly when delayed reconstruction is performed, shorter vascular pedicle requirement when compared to the thoracodorsal–subscapular system, better (less lateral) flap positioning, no risk of pedicle stretching from arm and shoulder movement and the location is convenient for a surgeon and an assistant to operate together under a microscope.

Main drawbacks of using internal mammary vessels are it may require extra time and dissection in immediate reconstruction, may necessitate partial rib excision and the IMA cannot be used as conduit for future coronary revascularisation.[36]

Anatomy. The IMA comes off the first part of the subclavian artery, and travels inferiorly and posterior to the brachiocephalic vein, then medial to the scalenus anterior muscle along the internal surface of the ribs. The artery can be located about 15 mm lateral to the sternal margin.[34] Between the sixth and seventh costal cartilage, the IMA divides into superior epigastric and musculophrenic arteries. The diameter of the IMA is between 1–2.5 mm, and tends to be larger on the right side.[34] The IMA is accompanied by at least one vein, but the venous anatomy can vary.

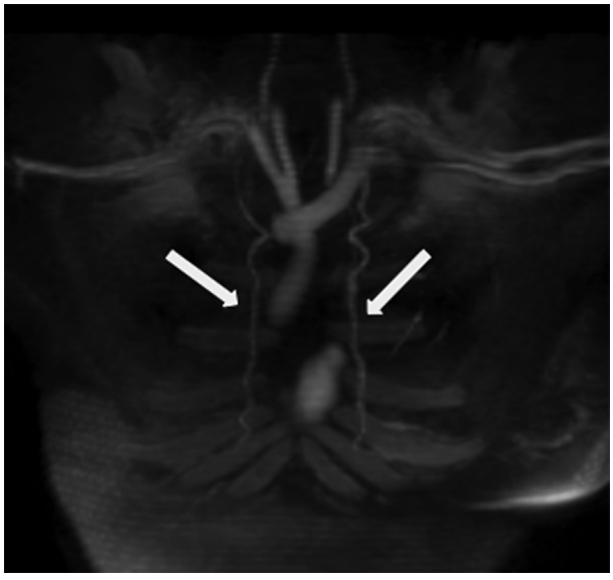

Figure 10 Coronal arterial phase images derived from spiral K space acquisition and sliding window reconstruction show patency in bilateral IMAs (arrows) post-autologous breast reconstruction. Note clip artefacts obscuring the anastomosis (arrowheads).

The internal mammary vein (IMV) is formed from the superior epigastric vein. It accompanies the IMA, and terminates into the brachiocephalic vein. The most common anatomy seen is an IMV coursing medial to the IMA (about 95% of patients). The medial IMV divides into two venae comitantes at the level of the third or fourth intercostals space in about 75% of patients.[37] The IMV may also divide into two venae comitantes at a higher or lower intercostal level.

Direct perforators arising from the IMA to the breast and skin at each intercostal space can be a recipient option to the internal mammary vessels[34]; however, in our experience, the internal mammary perforators are usually smaller calibre so do not match up well with the donor vessels, and the internal mammary vessels keep the breast skin alive, so transecting them in order to do an anastomosis may increase breast skin necrosis with mastectomy.

Imaging the internal mammary vessels. A patient is positioned prone to reduce respiratory motion. The imaging protocol is similar to donor site preoperative imaging, and includes axial and coronal T2-weighted images, precontrast, dynamic, and contrast-enhanced axial SPGR sequences, and contrast-enhanced coronal and sagittal SPGR sequences. High temporal resolution dynamic imaging in the coronal plane with spiral K space acquisition and sliding window reconstruction can isolate the arterial phase for evaluation of the patency of IMAs (Fig 10).

Reporting the recipient vessels. The diameter and patency of the IMA at the level of fourth rib is reported. The location of the IMA in relation to the IMV is reported. The distance of the IMA/IMV from the lateral margin of the sternum is reported. The costal level, at which the IMV divides into a medial and lateral venae comitante, is reported. Anatomical variations of IM vessels or pathological changes from vasculitides should be reported. Peri-arterial fibrosis and IMV thickening may be a consequence of adjunctive radiation treatment. In addition, prior surgeries may have damaged the vessels.[34] The IMA branches into perforators that supply the nipple–areolar complex (NAC). These perforators that supply the NAC may branch off at different intercostal levels, and the level can be reported.[38] In a nipple preserving mastectomy patient, a surgeon may use the information to access the internal mammary vessels more cephalad or caudal to preserve the perforator supplying the NAC. It is possible to anastomose a flap pedicle to an internal mammary perforator, but usually the perforator calibre is small, and not a good size match with the flap pedicle, resulting in more difficult anastomosis, and potential thrombosis.

Preoperative knowledge of the anatomy of the internal mammary vessels can direct the surgeon to access the internal mammary vessels at a specific intercostal level. Confirmation of patent internal mammary vessels is especially important in delayed reconstructions with adjuvant radiation therapy.[34] The thoracodorsal vessels patency and diameter are also reported because they are a second choice recipient vessel option.

Ionising radiation is an established breast cancer risk factor. Patients with primary breast cancer also carry a two to six-times higher risk of contralateral breast cancer than

the general population with a 10 year incidence of 10.5%.[39] Hence preoperative CTA of the chest may not be a preferred imaging method due to the risk of exposure of the contralateral breast to radiation and also radiation exposure to adjacent thyroid gland.[40] We anticipate MRA will increasingly be the method of choice for preoperative imaging of perforator flaps.

Postoperative imaging

The role of imaging in perforator flap reconstruction does not stop at preoperative mapping. A small number of patients require postoperative imaging of the reconstructed breast. The indication for post-reconstruction imaging is usually pain or a palpated firm mass on physical examination, with a clinical differential diagnosis of ischemic fat necrosis versus recurrent cancer. These patients can be imaged with mammogram and ultrasound if cleared by the surgeon. Patients that have a history of flap failure or partial flap failure with fat necrosis may be referred for further MRA imaging evaluation of the recipient vessels and/or donor site options (Fig 9a).

Imaging the postoperative chest

Patients are positioned prone to reduce respiratory motion. The imaging protocol is very similar to the preoperative imaging protocol, and includes axial and coronal T2 weighted images, precontrast, dynamic, and contrast-enhanced axial SPGR sequences, and contrast-enhanced coronal and sagittal SPGR sequences. A high temporal resolution dynamic imaging in the coronal plane with spiral K space acquisition and sliding window reconstruction is used to isolate the arterial phase for evaluation of the patency of the IMAs (Fig 10). A limitation to imaging is if there is a clip that causes artefact and obscures the vessels. This clip artefact may be exacerbated by spiral imaging. Flap enhancement on the precontrast images is subtracted from the dynamic and contrast-enhanced images to help determine areas of flap necrosis. TDAP and large intercostal artery perforators are also reported because the mid-back may yield adequate tissue for breast flap revision (Fig 9).

Tissue expander and MRI

Post-mastectomy patients referred for preoperative MRA mapping may have a tissue expander with a magnetic port (Electronic Supplementary Material Fig S1). These expanders are presently labelled “MR unsafe” because of concern for tissue migration and heat generation during MRI[41]; however, recent studies have demonstrated that the magnetic field interactions of most commercially available expanders are not significant and hence will not pose a risk to a patient in a magnetic field equivalent to or less than 3 T.[42] The same article reported that the highest temperature rise was 1.7°C, which is considered physiologically inconsequential.[42] In addition, the tissue expander in this population is intended to be removed at the time of autologous reconstruction, shortly after MRA. Thus, the risk of migration (tissue expander rotating or flipping in the scar capsule) or tissue expander damage is acceptable to the patient and surgeon because the risks associated with an additional surgery to remove the tissue expander prior to MRI far outweighs the relatively minimal risks of MRI scanning with the tissue expander in place.[41] The downside of tissue expanders is the substantial artefact created in the chest area. MRA evaluation of donor site perforator anatomy is usually far enough from chest artefact created by a tissue expander.[41]

Risks associated with MRI of patients with tissue expanders can be alleviated by: 1) giving the expander a potentially final fill just before MRI (in case the tissue expander is affected by the MRI and can no longer be filled); 2) scanning in the prone position; 3) scanning at 1.5 T or lower field strength; 4) giving the patient a squeeze ball to activate an alarm if there are any symptoms related to the expanders so the patient can be pulled out of the scanner quickly; 5) obtaining written informed consent.[41]

Automation of reporting

A preoperative perforator flap angiography report typically provides precise perforator coordinates, diameter, course, and estimated flap volume of more than one donor site region of the body. Manual measurements and report creation can take hours and potentially lead to workflow issues. Several software innovations, including OsiriX for 3D mapping of the perforator arteries have been reported.[43,44] An OsiriX-based automated plugin was developed exclusively for perforator mapping by our team at Weill Cornell Medical Center and is available for free download (http://github.com/cjlange/pfara/releases) (Electronic Supplementary Material Fig S2). The automatic perforator reporting software has been implemented as an OsiriX DICOM viewer plugin, and assists in measuring and reporting perforator and reference point coordinates, perforating vessel course and length beginning at the muscle–fat interface. This perforator software is routinely used in clinical reporting and has reduced the radiology reporting time threefold.[45]

Advantages of the automated system include significant reduction in reporting time for the radiologist, low-cost, familiarity of the radiologists and surgeons with Macintosh interface, promotion of uniform reporting style, reporting more perforators because of the decreased effort (which potentially provides more perforator choices), and elimination of manual transcription errors. Presently, at our institution preliminary reports are generated by radiology assistants using the automated software, which are reviewed later by supervising radiologists.[45]

Other benefits of preoperative mapping

Preoperative flap MRI can also detect unexpected pathology. In 551 patients who underwent MRA for preoperative imaging between September 2011 to December 2014 at our institution, MRA detected hepatic or bone metastases in seven patients[12] (Fig 2). Other pathology detected were

pancreatic cysts, gallbladder stones, hepatic steatosis, and gonadal vein thrombosis.

Conclusion

For nearly a decade, MRA is the first choice imaging test at our centre for preoperative evaluation of patients for autologous breast reconstruction. Visualising multiple donor sites in one study guides surgical approach and reduces operative time, which contributes to a successful reconstruction. The preoperative knowledge of MRA findings allows surgeons to accurately counsel patients preoperatively for realistic options for donor site selection. Furthermore, MRA helps greatly in the overall safety in intraoperative surgical dissection and decision-making as well as a potential postoperative failure second flap options. Continuous optimisation of protocols and post-processing techniques has been done to keep up with the advances in microsurgery reconstruction techniques and surgical reconstruction options. Pre- and postoperative MRA of the chest has the potential to guide surgical approach, reduce operative time and complication rate.

Conflict of interest

None.

Appendix A. Supplementary data

Supplementary data related to this article can be found at https://doi.org/10.1016/j.crad.2017.12.018.

References

1. Elder EE, Brandberg Y, Björklund T, *et al*. Quality of life and patient satisfaction in breast cancer patients after immediate breast reconstruction: a prospective study. *Breast* 2005;**14**:201–8.
2. Murphy Jr RX, Wahhab S, Rovito PF, *et al*. Impact of immediate reconstruction on the local recurrence of breast cancer after mastectomy. *Ann Plast Surg* 2003;**50**:333–8.
3. Handel N, Cordray T, Gutierrez J, Jensen AJ. A long-term study of outcomes, complications, and patient satisfaction with breast implants. *Plast Reconstr Surg* 2006 Mar;**117**(3):757–67. discussion 768-72.
4. FDA. Breast implants. Available at: https://www.fda.gov:80/FDAgov/MedicalDevices/ProductsandMedicalProcedures/ImplantsandProsthetics/BreastImplants/ucm239996.htm. Accessed 11/01/2017.
5. Leberfinger AN, Behar BJ, Williams NC, *et al*. Breast implant-associated anaplastic large cell lymphoma: a systematic review. *JAMA Surg* 2017 Dec 1;**152**(12):1161–8.
6. Allen RJ, Treece P. Deep inferior epigastric perforator flap for breast reconstruction. *Ann Plast Surg* 1994 Jan;**32**(1):32–8.
7. Vasile J. Perforator flap microsurgical breast reconstruction. Available at: http://www.julievasilemd.com/pages/breast-reconstruction. Accessed 09/09/2017.
8. The Center for Microsurgical Breast Reconstruction. Perforator flaps in breast reconstruction. Available at: https://www.diepflap.com/articles/perforator-flaps-in-breast-reconstruction. Accessed 09/09/2017.
9. Pratt GF, Rozen WM, Chubb D, *et al*. Preoperative imaging of perforator flaps in reconstructive surgery: a systematic review of the evidence for current techniques: reply. *Ann Plast Surg* 2013 Aug;**71**(2):2467.
10. Greenspun D, Vasile J, Levine JL, *et al*. Anatomic imaging of abdominal perforator flaps without ionizing radiation: seeing is believing with magnetic resonance imaging angiography. *J Reconstr Microsurg* 2010 Jan;**26**(1):37–44.
11. Lee JS, Patel KM, Zou Z, *et al*. Computerized tomographic and magnetic resonance angiography for perforator-based free flaps: technical considerations. *Clin Plast Surg* 2011 Apr;**38**(2):219–28.
12. Thimmappa N, Dutruel SP, Pei M, *et al*. Pre-operative perforator flap imaging for autologous reconstructive breast surgeries. *Proc ISMRM* 2013;**8**:4465.
13. Agrawal MD, Thimmappa ND, Vasile JV, *et al*. Autologous breast reconstruction: preoperative magnetic resonance angiography for perforator flap vessel mapping. *J Reconstr Microsurg* 2015 Jan;**31**(1):1–11.
14. Lewis M, Yanny S, Malcolm PN. Advantages of blood pool contrast agents in MR angiography: a pictorial review. *J Med Imaging Radiat Oncol* 2012 Apr;**56**(2):187–91.
15. Zou Z, Lee KH, Levine JL, *et al*. Gadofosveset trisodium-enhanced abdominal perforator MRA. *J Magn Reson Imaging* 2012 Mar;**35**(3):711–6.
16. Coroneos CJ, Heller AM, Voineskos SH, *et al*. SIEA versus DIEP arterial complications: a cohort study. *Plast Reconstr Surg* 2015 May;**135**(5):802e–7e.
17. Tseng CY, Lipa JE. Perforator flaps in breast reconstruction. *Clin Plast Surg* 2010 Oct;**37**(4):641–54. vi-ii.
18. Granzow JW, Levine JL, Chiu ES, *et al*. Breast reconstruction with the deep inferior epigastric perforator flap: history and an update on current technique. *J Plast Reconstr Aesthet Surg* 2006;**59**(6):571–9.
19. Fukaya E, Kuwatsuru R, Iimura H, *et al*. Imaging of the superficial inferior epigastric vascular anatomy and preoperative planning for the SIEA flap using MDCTA. *J Plast Reconstr Aesthet Surg* 2011 Jan;**64**(1):63–8.
20. Kim D-Y, Lee TJ, Kim EK, *et al*. Intraoperative venous congestion in free transverse rectus abdominis musculocutaneous and deep inferior epigastric artery perforator flaps during breast reconstruction: a systematic review. *Plast Surg* 2015;**23**(4):255–9.
21. Rozen WM, Ashton MW. The venous anatomy of the abdominal wall for deep inferior epigastric artery (DIEP) flaps in breast reconstruction. *Gland Surg* 2012;**1**(2):92–110.
22. Schaverien MV, Ludman CN, Neil-Dwyer J, *et al*. Relationship between venous congestion and intraflap venous anatomy in DIEP flaps using contrast-enhanced magnetic resonance angiography. *Plast Reconstr Surg* 2010 Aug;**126**(2):385–92.
23. Taylor GI, Townsend P, Corlett R. Superiority of the deep circumflex iliac vessels as the supply for free groin flaps. Clinical work. *Plast Reconstr Surg* 1979;**64**:745–59.
24. Vasile JV, Levine JL. Magnetic resonance angiography in perforator flap breast reconstruction. *Gland Surg* 2016 Apr;**5**(2):197–211.
25. Hendricks HP, Ingianni G, Bohm E, *et al*. Microvascular peritoneal flap based on the deep circumflex iliac artery—an anatomic study. *Eur J Plast Surg* 1995;**18**:88–90.
26. Bergeron L, Tang M, Morris SF. The anatomical basis of the deep circumflex iliac artery perforator flap with iliac crest. *Plast Reconstr Surg* 2007;**120**:252–8.
27. Buchel E. Deep circumflex iliac artery perforator flap for breast reconstruction. In: Levine JL, Vasile CM Chen J, Allen RJ, editors. *Perforator flaps for breast reconstruction*. New York: Thieme; 2016.
28. Rozen WM, Ting JW, Grinsell D, *et al*. Superior and inferior gluteal artery perforators: *in vivo* anatomical study and planning for breast reconstruction. *J Plast Reconstr Aesthet Surg* 2011 Feb;**64**(2):217–25.
29. Ahmadzadeh R, Bergeron L, Tang M, *et al*. The superior and inferior gluteal artery perforator flaps. *Plast Reconstr Surg* 2007 Nov;**120**(6):1551–6.
30. Allen RJ, Haddock NT, Ahn CY, *et al*. Breast reconstruction with the profunda artery perforator flap. *Plast Reconstr Surg* 2012 Jan;**129**(1):16e–23e.
31. Ahmadzadeh R, Bergeron L, Tang M, *et al*. The posterior thigh perforator flap or profunda femoris artery perforator flap. *Plast Reconstr Surg* 2007 Jan;**119**(1):194–200.
32. Peters KT, Blondeel PN, Lobo F, *et al*. Early experience with the free lumbar artery perforator flap for breast reconstruction. *J Plast Reconstr Aesthet Surg* 2015 Aug;**68**(8):1112–9.
33. Jain L, Kumta SM, Purohit SK, *et al*. Thoracodorsal artery perforator flap: Indeed a versatile flap. *Indian J Plast Surg* 2015 May-Aug;**48**(2):153–8.
34. Murray AC, Rozen WM, Alonso-Burgos A, *et al*. The anatomy and variations of the internal thoracic (internal mammary) artery and implications in autologous breast reconstruction: clinical anatomical study and literature review. *Surg Radiol Anat* 2012 Mar;**34**(2):159–65.

35. O'Neill AC, Hayward V, Zhong T, *et al*. Usability of the internal mammary recipient vessels in microvascular breast reconstruction. *J Plast Reconstr Aesthet Surg* 2016 Jul;**69**(7):907–11.
36. Quaba O, Brown A, Stevenson H. Internal mammary vessels, recipient vessels of choice for free tissue breast reconstruction? *Br J Plast Surg* 2005 Sep;**58**(6):881–2.
37. Arnez ZM, Valdatta L, Tyler MP, *et al*. Anatomy of the internal mammary veins and their use in free TRAM flap breast reconstruction. *Br J Plast Surg* 1995 Dec;**48**(8):540–5.
38. Stirling AD, Murray CP, Lee MA. The arterial supply of the nipple areola complex (NAC) and its relations: an analysis of angiographic CT imaging for breast pedicle design. *Surg Radiol Anat* 2017 Oct;**39**(10):1127–34.
39. Rubino C, Arriagada R, Delaloge S, *et al*. Relation of risk of contralateral breast cancer to the interval since the first primary tumour. *Br J Cancer* 2010;**102**(1):213–9.
40. Rozen WM, Alonso-Burgos A, Murray AC, *et al*. Is there a need for preoperative imaging of the internal mammary recipient site for autologous breast reconstruction? *Ann Plast Surg* 2013 Jan;**70**(1):111–5.
41. Thimmappa ND, Prince MR, Colen KL, *et al*. Breast tissue expanders with magnetic ports: clinical experience at 1.5 T. *Plast Reconstr Surg* 2016 Dec;**138**(6):1171–8.
42. Linnemeyer H, Shellock FG, Ahn CY. *In vitro* assessment of MRI issues at 3-Tesla for a breast tissue expander with a remote port. *Magn Reson Imaging* 2014 Apr;**32**(3):297–302.
43. Chae MP, Hunter-Smith DJ, Rozen WM. Comparative study of software techniques for 3D mapping of perforators in deep inferior epigastric artery perforator flap planning. *Gland Surg* 2016;**5**(2):99–106.
44. Eder M, Raith S, Jalali J, *et al*. Three-dimensional prediction of free-flap volume in autologous breast reconstruction by CT angiography imaging. *Int J Comput Assist Radiol Surg* 2014;**9**(4):541–9.
45. Lange CJ, Thimmappa ND, Boddu SR, *et al*. Automating perforator flap MRA and CTA reporting. *J Digit Imaging* 2017 Jun;**30**(3):350–7.